Tertiary Conformation of the Template-Primer and Gapped DNA Substrates in Complexes with Rat Polymerase β. Fluorescence Energy Transfer Studies Using the Multiple Donor−Acceptor Approach†

Maria J. Jezewska, Roberto Galletto, and Wlodzimierz Bujalowski*

Department of Human Biological Chemistry and Genetics and Sealy Center for Structural Biology, The University of Texas Medical Branch at Galveston, 301 University Boulevard, Galveston, Texas 77555-1053

Received May 2, 2003

ABSTRACT: The tertiary structure of template-primer and gapped DNA substrates in the complex with rat polymerase β (pol β) has been examined using the fluorescence energy transfer method based on the multiple donor−acceptor approach. In these studies, we used DNA substrates labeled at the 5′ end of the template strand and the 5′ end of the primer with the fluorescent donor and/or acceptor. Measurements of the enzyme complex with the template-primer DNA substrate having a ten nucleotide long ssDNA extension indicate that the distance between the 5′ end of the template strand and the 5′ end of the primer decreases by ∼9.8 Å as compared to the free nucleic acid. Analogous experiments with the template-primer substrate, having the ssDNA extension with five nucleotide residues, show ∼6.6 Å distance decrease. Such large distance decreases indicate that the DNA is significantly bent in the binding site. Analysis of the data indicates that the bending occurs between the third and the fourth nucleotide of the ssDNA extension. The entire template strand is at the bend angle $\Theta_{TP} = 85 \pm 7°$ with respect to the dsDNA part of the DNA molecule. In the polymerase complex with the gapped DNA, the distance between the 5′ ends of the DNA and the bend angle are 66 ± 2.2 Å and $65 \pm 6°$, respectively. These values are very similar to the same distance and bend angle of the gap complex in the crystal structure of the co-complex. The presence of the 5′-terminal PO_4^- group downstream from the primer does not affect the tertiary conformation of the gapped DNA, indicating that the effect of the phosphate group is localized at the ssDNA gap.

One of the fundamental steps in the DNA repair process is the recognition of specific structures of damaged DNAs by a DNA repair polymerase (*1*−*9*). This recognition process must precede the chemical step of the DNA synthesis. Several DNA polymerases in the mammalian cell are engaged in the DNA repair processes, including polymerase β (pol β) that is involved in gap-filling synthesis in mismatch repair, repair of monofunctional adducts, UV-damaged DNA, and abasic lesions in DNA (*1*−*7*). The complexity of the DNA recognition process by pol β is reflected in the complexity of its total DNA-binding site. The total binding site is built of two DNA-binding subsites, each located on a different structural domain of the enzyme, the small 8 kDa and the large 31 kDa catalytic domains (*7*, *8*−*11*). Similar domain arrangement has been proposed for other DNA polymerases engaged in DNA repair (*12*−*15*). Both the 8 and 31 kDa domains have DNA-binding capability; however, only the 8 kDa domain has similar affinity for both, the ssDNA and dsDNA (*16*, *17*). This is particularly evident in the enzyme binding to the template-primer (TP)[1] and gapped DNA substrates (*10*, *11*).

Spatial separation of the two DNA-binding subsites of the polymerase, located on two structurally different domains, with very different DNA-binding capabilities, results in a very complex DNA-binding mechanism of both human and rat pol β (*8*−*11*). The enzymes bind the ssDNA in two binding modes that differ in the number of occluded nucleotide residues, the $(\text{pol }\beta)_{16}$ and the $(\text{pol }\beta)_5$ binding mode (*8*, *9*). In the $(\text{pol }\beta)_{16}$ binding mode, both the 8 and the 31 kDa domains are involved in interactions with the ssDNA; i.e., the total DNA-binding site of the enzyme is engaged in the complex. An analogous complex is formed with the template-primer substrates where the 8 kDa domain engages the ssDNA part and the 31 kDa domain binds the dsDNA part of the substrate, forming a template-primer complex (*10*, *11*). The high affinity of formed complexes results from anchoring the polymerase on the DNA with both domains involved in interactions with different nucleic acid conformations. On the other hand, in the $(\text{pol }\beta)_5$ binding mode, only the 8 kDa domain is engaged in interactions with the DNA.

Formation of different binding modes with the ssDNA and the template-primer complex indicates significant autonomy as well as a sophisticated communication mechanism between the two DNA-binding subsites of pol β (*8*−*11*). This is evident in kinetic analyses of human and rat pol β interactions with the ssDNA in the $(\text{pol }\beta)_{16}$ and $(\text{pol }\beta)_5$ binding modes and the recognition of the gapped DNA

† This work was supported by NIH Grant GM-58565 (to W.B.).

* To whom correspondence should be addressed. Tel: (409) 772-5634. Fax: (409) 772-1790. E-mail: wbujalow@utmb.edu.

[1] Abbreviations: DTT, dithiothreitol; CP, 7-(diethylamino)-3-(4′-maleimidylphenyl)-4-methylcoumarin; Flu, fluorescein; Rho, rhodamine; bps, base pairs; TP, template-primer.

10.1021/bi030111l CCC: $25.00
Published on Web 09/20/2003

substrates by the enzymes (*18*−*21*). Formation of ssDNA binding modes and binding of the polymerase to gapped DNAs are initiated through the very fast, diffusion-controlled, association of the DNA-binding subsite located on the 8 kDa domain. Only then, in several sequential steps, induced by the conformational transitions at the protein−DNA interface on the 8 kDa domain and controlled by ion binding, the 31 kDa domain engages in interactions with the nucleic acid, leading to the formation of the (pol β)$_{16}$ binding mode or gap complex (*18*−*21*).

Although the crystal structures of co-complexes with the ssDNA are not available and the resolution of template-primer complex does not allow exact determination of the positioning of the template strand, the crystal structure of the gap complex shows strong bending of the DNA molecule in the binding site of pol β (*7*). This strongly suggests that the template strand of the template-primer DNA is also bent with respect to the dsDNA part of the nucleic acid. Moreover, spectroscopic data indicate that the engagement of the total binding site of pol β in interactions with the DNA in the (pol β)$_{16}$ binding mode, template-primer, or gap complex involves not only conformational transitions of the protein but also profound changes in the nucleic acid structure (*8*−*11*, *18*−*21*). Elucidation of DNA conformational changes accompanying the formation of the complex with pol β in solution is one of the fundamental steps toward understanding the molecular mechanism of the DNA recognition by pol β and other DNA repair polymerases. Despite its paramount importance for understanding the DNA recognition process, the direct analysis of DNA substrate conformation in the complex with pol β in solution has not yet been addressed.

In this paper, we report fluorescence energy transfer studies of the tertiary structure of template-primer and gapped DNA substrates in the complex with rat pol β in solution, using the multiple donor−acceptor approach (*22*−*25*). We present direct evidence that binding of the template-primer DNA substrate to the enzyme induces a large decrease in the distance between the 5′ end of the template strand and the 5′ end of the primer, indicating that the DNA substrate is significantly bent in the total DNA-binding site of the enzyme. The data indicate that the entire ssDNA of the template strand is bent at a single location in the ssDNA extension. The conformation of the gapped DNA in the complex with pol β is very similar to the crystal structure of the co-complex. The presence of the 5′-terminal PO_4^- group downstream from the primer does not affect the tertiary conformation of the bound gapped DNA.

MATERIALS AND METHODS

Reagents and Buffers. All solutions were made with distilled >18 MΩ (Milli-Q Plus) water. All chemicals were of reagent grade. Buffer C is 10 mM sodium cacodylate adjusted to pH 7.0 with HCl, 10% glycerol, and 1 mM DTT. The temperatures and concentrations of NaCl and $MgCl_2$ in the buffer are indicated in the text.

Rat Polymerase β. Rat pol β was purified as previously described (*8*−*11*). The concentration of the protein was determined using the extinction coefficient $\epsilon_{280} = 2.1 \times 10^4$ cm^{-1} M^{-1} obtained using the method based on Edeldoch's approach (*8*, *26*−*28*).

Nucleic Acids. All nucleic acids were purchased from Midland Certified Reagents (Midland, TX). The oligomers, labeled with fluorescein at the 5′ end, were synthesized using fluorescein phosphoramidate. Labeling with rhodamine (Rho) or coumarin (CP) was performed by synthesizing and modifying DNA oligomers with a nucleotide residue having the amino group on a six-carbon linker. The degree of labeling was determined by absorbance, using the extinction coefficients $\epsilon_{494} = 7.6 \times 10^4$ M^{-1} cm^{-1} (pH 9), $\epsilon_{436} = 4.4 \times 10^4$ M^{-1} cm^{-1}, and $\epsilon_{555} = 8.0 \times 10^4$ M^{-1} cm^{-1} for fluorescein, coumarin, and rhodamine (*22*−*24*). Concentrations of all ssDNA oligomers have been spectrophotometrically determined as previously described (*22*−*24*). Template-primer and gap DNA substrates were obtained by mixing proper oligomers at given concentrations, warming up the mixture for 5 min at 95 °C, and slowly cooling for a period of ∼3−4 h. Integrity of all substrates has been checked using UV melting and analytical ultracentrifugation techniques (*22*−*24*).

Steady-State and Time-Dependent Fluorescence Measurements. All steady-state fluorescence titrations were performed using the SLM-AMINCO 8100 spectrofluorometer as previously described (*8*−*11*, *18*−*26*, *29*). To avoid possible artifacts, due to the fluorescence anisotropy of the sample, polarizers were placed in excitation and emission channels and set at 0° and 54.7° (magic angle), respectively (*30*). The emission spectra have been corrected for instrument characteristics using the software provided by the manufacturer. Time-dependent fluorescence lifetime and anisotropy measurements have been performed using an IBH 5000U time-correlated single photon counting instrument (IBH, Glasgow, U.K.) equipped with polarizers as well as excitation and emission monochromators. Excitations were performed with nanosecond light emitting diodes at 450, 495, and 560 nm for coumarin, fluorescein, and rhodamine. Glycogen solution was used as a reference for the excitation source profile. Analyses of anisotropy decay curves were performed using the nonlinear, least-squares software provided by the manufacturer.

Determination of the Average Fluorescence Energy Transfer Efficiency from a Donor to an Acceptor Located on the DNA Substrates. The apparent efficiency of the fluorescence radiationless energy transfer, E, from a donor to an acceptor located on a DNA substrate has been determined using two independent methods. The fluorescence of the donor in the presence of the acceptor, F_{DA}, is related to the fluorescence of the same donor, F_D, in the absence of the acceptor by (*22*−*24*)

$$F_{DA} = (1 - \nu_D)F_D + F_D\nu_D(1 - E_D) \qquad (1)$$

where ν_D is the fraction of donors in the complex with the acceptor and E_D is the average fluorescence energy transfer efficiency determined using the donor emission quenching. The quantity, E_D, is then

$$E_D = \left(\frac{1}{\nu_D}\right)\left(\frac{F_D - F_{DA}}{F_D}\right) \qquad (2)$$

The values of ν_D have been obtained using the binding constants of a given DNA substrate for the rat pol β measured in the same solution conditions (see below).

In the second independent method, the average fluorescence transfer efficiency, E_A, is obtained by sensitized

acceptor fluorescence. This can be accomplished by measuring the fluorescence intensity of the acceptor, excited at a wavelength where a donor predominantly absorbs, in the absence and presence of the donor. The fluorescence intensities of the acceptor in the absence, F_A, and presence, F_{AD}, of the donor are defined as

$$F_A = I_o \epsilon_A C_{AT} \phi_F^A \quad (3)$$

and

$$F_{AD} = (1 - \nu_A)F_A + I_o \epsilon_A \nu_A C_{AT} \phi_B^A + I_o \epsilon_D C_{DT} \nu_D \phi_B^A E_A \quad (4)$$

where I_o is the intensity of incident light, C_{AT} and C_{DT} are the total concentrations of acceptor and donor, ν_A is the fraction of acceptors in the complex with donors, ϵ_A and ϵ_D are the molar absorption coefficients of acceptor and donor at the excitation wavelength, respectively, and ϕ_F^A and ϕ_B^A are the quantum yields of the free and bound acceptor. All quantities in eqs 3 and 4 can be experimentally determined (*22*−*24*). For the case considered in this work, the acceptor is practically completely saturated with the donor; i.e., $\nu_A = 1$. Thus, for $\nu_A = 1$, dividing eq 4 by 3 and rearranging provides the average transfer efficiency as described by

$$E_A = \left[\frac{1}{\nu_D}\right]\left(\frac{\epsilon_A C_{AT}}{\epsilon_D C_{DT}}\right)\left[\left(\frac{\phi_F^A}{\phi_B^A}\right)\left(\frac{F_{AD}}{F_A}\right) - 1\right] \quad (5)$$

As mentioned above, the energy transfer efficiencies, E_D and E_A, are apparent quantities. E_D is a fraction of photons absent in the donor emission as a result of the presence of an acceptor, including transfer to the acceptor and possible nondipolar quenching processes induced by the presence of the acceptor, and E_A is a fraction of all photons absorbed by the donor which were transferred to the acceptor. The true Förster energy transfer efficiency, E, is a fraction of the photons absorbed by the donor and transferred to the acceptor, in the absence of any additional nondipolar mechanism (*31*). The value of E is related to the apparent quantities of E_D and E_A by (*32*)

$$E = \frac{E_A}{1 - E_D + E_A} \quad (6)$$

Thus, measurements of the transfer efficiency, using both methods, are not alternatives but parts of the entire analysis used to obtain the true efficiency of the fluorescence energy transfer process, E.

The fluorescence energy transfer efficiency between the donor and acceptor dipoles is related to the distance, R, separating the dipoles by (*31*)

$$R = R_o\left(\frac{1 - E}{E}\right)^{1/6} \quad (7a)$$

and

$$R_o = 9790(\kappa^2 n^{-4} \phi_d J)^{1/6} \quad (7b)$$

where R_o is the so-called Förster critical distance (in angstroms), the distance at which the transfer efficiency is 50%, κ^2 is the orientation factor, ϕ_d is the donor quantum yield in the absence of the acceptor, and n is the refractive index of the medium ($n = 1.4$) (*31*). The overlap integral, J, characterizes the resonance between the donor and acceptor dipoles (*31*). The Förster critical distances, R_o, for the examined donor−acceptor pairs, have been determined before (*24*). The obtained values are 47 Å for coumarin−rhodamine, 52 Å for coumarin−fluorescein, and 54 Å for fluorescein−rhodamine pairs.

Multiple Donor−Acceptor Approach. The fluorescence energy transfer efficiency determined for chemically identical donor−acceptor pairs depends on the distance between the donor and the acceptor, R, and factor κ^2, describing the mutual orientation of the donor and acceptor dipoles (*31*−*33*). The factor κ^2 cannot be experimentally determined, although, because the distance between a donor and an acceptor depends on the $^1/_6$th power of κ^2, only the two extreme values (0 or 4) would strongly affect the determined distance. For completely random orientations of the donor and the acceptor, $\kappa^2 = 0.67$. The rigorous analysis of the possible range of distances between the donor and the acceptor has been developed for the situation where only a single donor−acceptor pair is used, by examining limiting anisotropies of the macromolecular system for both the donor and the acceptor (*33*). However, another rigorous procedure to evaluate the error in the distance determination is to use multiple donor−acceptor pairs and their interchanged locations (*24*). This approach introduces the required intrinsic randomization of the orientation of the absorption and emission dipoles in the studied system. The measurement of similar distances using multiple donor−acceptor pairs indicates that the obtained average distance between the donor and the acceptor is not affected by the extreme values of κ^2 (see below).

Quantum Yield Determinations. The quantum yields of different chromophores used in this work, ϕ, were determined by the comparative method (*34*, *35*) previously described (*22*−*24*). Quinine bisulfate in 0.1 N H_2SO_4 and fluorescein in 0.1 NaOH were used as a standard (absolute quantum yield $\phi = 0.7$ and 0.92, respectively) (*31*, *36*).

RESULTS

Binding of Rat Pol β to Template-Primer DNA Substrates. Formation of the Template-Primer Complex. The two ssDNA binding modes, (pol β)$_{16}$ and (pol β)$_5$, which rat pol β forms with the ssDNA, differ by the number of the occluded nucleotide residues in the protein−nucleic acid complex (*8*, *9*). Moreover, the enzyme binds the dsDNA with significant affinity (*10*, *11*, *16*). As a result, association of pol β with DNA substrates containing both the ssDNA extension and the dsDNA part is a process that includes multiple polymerase molecules associated with the DNA (*10*, *11*). To reduce the complexity, interactions of rat pol β with DNA substrates having the ssDNA extension have been examined using substrates that can accommodate the enzyme only in the (pol β)$_5$ binding mode in the ssDNA extension. The template-primer DNA substrates, used in the examination of the nucleic acid structure in the complex with rat pol β, are depicted in Figure 1. The duplex part of each substrate, containing primer, is ten bps long and is located at the 3′ end of the template strand. At the 5′ end of the template

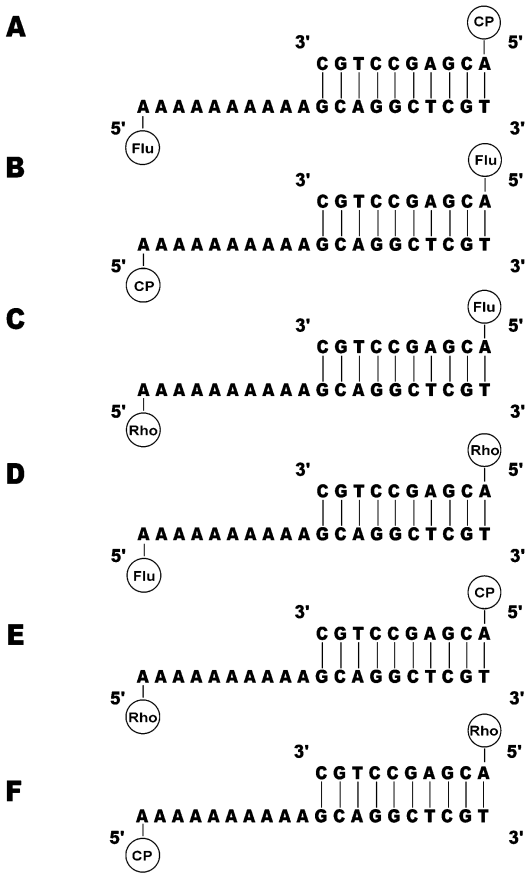

FIGURE 1: DNA substrates used in fluorescence energy transfer experiments to examine the conformation of the template-primer DNA substrate in the template-primer complex with rat pol β. The duplex parts of each substrate, containing the primer oligomer, are ten bps long. The ssDNA extensions have ten bases that allow the enzyme to bind only in the (pol β)$_5$ binding mode. At the 5′ end of the template strand and the primer, there is a fluorescence marker attached, coumarin (CP), fluorescein (Flu), and rhodamine (Rho), that serves as a donor or acceptor in the fluorescence energy transfer analyses (Materials and Methods). There are six possible arrangements of the selected three donor−acceptor pairs designated as substrates A, B, C, D, E, and F.

strand, there is a ten nucleotide residue long ssDNA extension, built of adenine nucleotides. The 5′ end of the template strand and the 5′ end of the primer oligomer are labeled with different fluorescent markers, fluorescein, coumarin, and rhodamine, that serve as donors or acceptors in the fluorescence energy transfer experiments described below. All six possible combinations of the donor−acceptor pairs used in the distance determinations are depicted in Figure 1. Thermodynamic studies showed that the presence of the different fluorescent labels does not affect the energetics of the enzyme binding to the DNA substrates to any detectable extent (data not shown). In other words, stoichiometries and intrinsic affinities of the polymerase with different nucleic acids, shown in Figure 1, are the same.

We have previously examined the quantitative thermodynamics of the rat pol β binding to the DNA substrates analogous to the ones depicted in Figure 1 (*10*, *11*). At saturation, three pol β molecules are bound to the DNA. At low and intermediate enzyme concentrations, the polymerase can form the high-affinity template-primer complex; i.e., the large 31 kDa domain is bound to the duplex part of the DNA substrate while the small 8 kDa domain engages the ssDNA of the template strand. Two enzyme molecules can bind the ssDNA extension in the (pol β)$_5$ binding mode. A single molecule of the polymerase can associate with the dsDNA part independently from the binding to the ssDNA extension (see below). However, we are interested only in the DNA structure in these complexes where the enzyme forms the functionally active template-primer complex, i.e., where the 3′ end of the primer is located in the active site of the DNA synthesis on the 31 kDa domain (*11*). The partition function, Z_{10}, of rat pol β−DNA substrate systems (Figure 1) is described by (*11*)

$$Z_{10} = 1 + (6K_5 + K_{DS} + K_{TP})P_F + (6K_5 + K_{DS} + \sigma K_5^2 + K_{DS}K_{TP})P_F^2 + \sigma K_5^2 K_{DS} P_F^3 \quad (8)$$

where K_5 is the intrinsic binding constant for the enzyme bound to the ssDNA extension in the (pol β)$_5$ binding mode, K_{DS} is the binding constant for the association with the dsDNA part, and K_{TP} is the binding constant characterizing the formation of the template-primer complex (*11*).

The molar fractional contributions of the free nucleic acid, Q_F, complexes containing template-primer complex, Q_{TP}, and all remaining complexes, Q_R, to DNA species in solution are

$$Q_F = \frac{1}{Z_{10}} \quad (9a)$$

$$Q_{TP} = \frac{K_{TP}P_F + K_{TP}K_{DS}P_F^2}{Z_{10}} \quad (9b)$$

and

$$Q_R = \frac{(6K_5 + K_{DS})P_F + (6K_5K_{DS} + \sigma K_5^2)P_F^2 + \sigma K_5^2 K_{DS} P_F^3}{Z_{10}} \quad (9c)$$

The values of all binding parameters have been obtained in independent fluorescence titration experiments (data not shown) which provided $K_5 = (8 \pm 2) \times 10^5$ M^{-1}, $K_{DS} = (2 \pm 0.6) \times 10^6$ M^{-1}, and $K_{TP} = (4 \pm 1.5) \times 10^7$ M^{-1}. As expected, these values are the same as the values obtained before for the analogous template-primer DNA substrates (*11*).

Using expressions 9a−c, one can estimate fractional contributions, Q_F, Q_{TP}, and Q_R, at selected concentrations of the nucleic acid, e.g., 3×10^{-7} M (oligomer). The contribution of the free DNA, Q_F, is undetectable at [rat pol β] reaching $\sim 1 \times 10^{-6}$ M. Above [rat pol β] $\sim 7 \times 10^{-7}$ M, complexes containing rat pol β bound in the template-primer configuration dominate the polymerase binding to the considered DNA substrates up to [rat pol β] $\sim 2 \times 10^{-6}$ M. The contribution of all other complexes to the total population of DNA species does not exceed 17% in this enzyme concentration range. However, as the enzyme concentration increases, the template-primer configuration begins to be replaced by the (pol β)$_5$ binding mode (*11*). At saturation, three rat pol β molecules are bound to the DNA substrate, two in the (pol β)$_5$ binding mode to the ssDNA extension and one to the dsDNA part. Thus, knowing the binding

parameters is crucial for the selection of the enzyme concentration that allows the optimal determination of the DNA structure in the template-primer complexes, i.e., where the contribution of the template-primer configuration to the population of DNA species dominates the molar fractional distribution. For the selected DNA concentration (3×10^{-7} M), the required total enzyme concentration is 9×10^{-7} M.

Average Distances between the 5′ End of the Template-Primer Strand and the 5′ End of the Primer in the Absence and Presence of Rat Pol β. Multiple Donor−Acceptor Experiments with the DNA Substrate Having a Ten Nucleotide Residue Long ssDNA Extension. The emission spectra ($\lambda_{ex} = 425$ nm) of the template-primer DNA substrate (Figure 1, substrate B) having only the donor (CP) at the 5′ end of the template strand and the same substrate having only the acceptor (Fl) at the 5′ end of the primer, in buffer C (pH 7.0, 10 °C) containing 100 mM NaCl and 1 mM $MgCl_2$, are shown in Figure 2a. The solid line in Figure 2a is the fluorescence emission spectrum of the DNA substrate containing both the donor and the acceptor at the same DNA concentration (Figure 1, substrate B). There are clear differences between the independent spectra of the nucleic acid with only the donor or acceptor and the spectrum where both donor and acceptor are placed on the same DNA substrate. The emission intensity of the donor (CP) at the maximum at 478 nm, in the presence of the acceptor on the same DNA molecule, is decreased by ~8%. The decrease of emission at 478 nm indicates a fluorescence energy transfer from the CP located at the 5′ end of the template strand to the fluorescein moiety located at the 5′ end of the primer.

Comparison between the independent spectra of the donor and acceptor and the spectrum of the double-labeled DNA substrate shows that the fluorescence intensity of the fluorescein residue, with the peak at ~520 nm, is significantly increased when the donor and acceptor are located on the same DNA molecule. Because fluorescein does not contribute to the CP emission band at 478 nm, we can normalize the spectrum of the donor to the spectrum of the double-labeled DNA substrate at 478 nm. The difference between the normalized spectrum of the donor and the spectrum of the double-labeled DNA provides the sensitized emission spectrum of the acceptor. The sensitized emission spectrum of the fluorescein in the double-labeled DNA substrate is shown in Figure 2a. In the presence of CP, the emission intensity of the fluorescein residue is increased ~2.3-fold.

The presence of rat pol β has a large effect on the fluorescence energy transfer from the donor to the acceptor in the considered template-primer DNA substrate. The emission spectra ($\lambda_{ex} = 425$ nm) of the DNA substrate containing only CP at the 5′ end of the template strand and the same substrate containing only fluorescein at the 5′ end of the primer in the presence of rat pol β, in buffer C (pH 7.0, 10 °C) containing 100 mM NaCl and 1 mM $MgCl_2$, are shown in Figure 2b. The concentration of the enzyme is 9×10^{-7} M. At this enzyme concentration, the template-primer complex dominates the distribution of the protein−DNA complexes (*11*). The solid line in Figure 2b is the emission spectrum of the DNA substrate containing both the donor and the acceptor in the presence of the polymerase, at the same enzyme and nucleic acid concentrations as used in recording the independent spectra. In the presence of rat pol β, the emission intensity at the donor of the double-labeled DNA substrate is decreased by ~23% as compared to 8% in the absence of the polymerase (Figure 2a). The emission spectrum of the double-labeled DNA substrate in the presence of the enzyme shows that the fluorescence intensity of the fluorescein residue at the 5′ end of the primer, with the peak at ~520 nm, is also increased to a much larger extent than observed for the same DNA substrate in the absence of the enzyme.

Similarly to the situation without rat pol β, we can normalize the spectrum of the donor, CP, to the spectrum of the double-labeled DNA substrate at 478 nm. The difference between the normalized spectrum of the donor and the

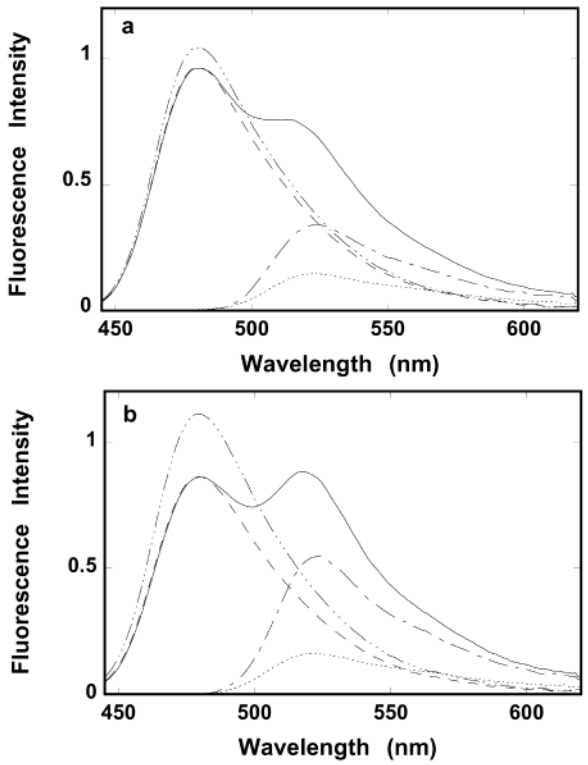

FIGURE 2: (a) Fluorescence emission spectrum ($\lambda_{ex} = 425$ nm) of the template-primer DNA substrate with CP at the 5′ end of the template strand (− --- −), the template-primer DNA substrate containing Fl at the 5′ end of the primer oligomer (---), and the template-primer DNA containing both CP and Fl (—) (Figure 1, substrate B) in buffer C (pH 7.0, 10 °C), containing 100 mM NaCl and 1 mM $MgCl_2$; the normalized emission spectrum of the template-primer DNA substrate, containing CP at the 5′ end of the template strand, to the maximum of the double-labeled DNA at 478 nm (− −); the sensitized emission of the template-primer DNA containing both CP at the 5′ of the template strand and Fl at the 5′ end of the primer oligomer (− - −). Concentrations of oligomers are 3×10^{-7} M. (b) Fluorescence emission spectrum ($\lambda_{ex} = 425$ nm) of the template-primer DNA substrate containing CP at the 5′ end of the template strand in the presence rat pol β (− --- −), the template-primer DNA substrate containing Fl at the 5′ end of the primer oligomer in the presence rat pol β (---), and the template-primer DNA containing both CP and Fl in the presence rat pol β (—) (Figure 1, substrate B) in buffer C (pH 7.0, 10 °C) containing 100 mM NaCl and 1 mM $MgCl_2$; the normalized emission spectrum of the template-primer DNA substrate, containing CP at the 5′ end of the template strand, to the maximum of the double-labeled DNA at 478 nm (− −); the sensitized emission of the template-primer DNA containing both CP and Fl (− - −). Concentrations of the rat pol β and template-primer DNA substrates are 9×10^{-7} and 3×10^{-7} M, respectively.

Table 1: Fluorescence Energy Transfer Parameters for Template-Primer DNA Substrates Having Ten Nucleotide Residues in the ssDNA Extension in the Absence and Presence of Rat Pol β in Buffer C (pH 7.0, 10 °C) Containing 100 mM NaCl and 1 mM $Mgcl_2$[a]

template-primer DNA (Figure 1)	E_D	E_A	E_{10}	E_{TP}	R^b (Å)	$R_{TP}{}^b$ (Å)
A	0.11 ± 0.01	0.12 ± 0.01	0.12 ± 0.01		72.5 ± 1.2	
B	0.08 ± 0.01	0.16 ± 0.01	0.15 ± 0.01		69.4 ± 1.2	
C	0.21 ± 0.01	0.20 ± 0.01	0.20 ± 0.01		68.0 ± 1.2	
D	0.23 ± 0.01	0.25 ± 0.01	0.24 ± 0.01		65.4 ± 1.2	
E	0.08 ± 0.01	0.12 ± 0.01	0.11 ± 0.01		66.6 ± 1.2	
F	0.1 ± 0.01	0.11 ± 0.01	0.11 ± 0.01		66.6 ± 1.2	
					R_{av}:[c] 68.1 ± 2.3	
A + rat pol β	0.23 ± 0.01	0.30 ± 0.01	0.28 ± 0.01	0.31 ± 0.01		59.4 ± 1.2
B + rat pol β	0.23 ± 0.01	0.27 ± 0.01	0.26 ± 0.01	0.28 ± 0.01		61.0 ± 1.2
C + rat pol β	0.34 ± 0.01	0.27 ± 0.01	0.29 ± 0.01	0.31 ± 0.01		61.7 ± 1.2
D + rat pol β	0.48 ± 0.01	0.29 ± 0.01	0.36 ± 0.01	0.38 ± 0.01		58.6 ± 1.2
E + rat pol β	0.31 ± 0.01	0.28 ± 0.01	0.29 ± 0.01	0.33 ± 0.01		53.0 ± 1.2
F + rat pol β	0.22 ± 0.01	0.23 ± 0.01	0.23 ± 0.01	0.26 ± 0.01		56.0 ± 1.2
						R_{TPav}:[c] 58.3 ± 3

[a] Details in the text. [b] The error is the standard deviation obtained from three to four independent experiments. [c] The error is the standard deviation determined using distances for all six DNA substrates.

spectrum of the double-labeled DNA provides the sensitized emission spectrum of the acceptor in the presence of rat pol β. The sensitized emission spectrum of the fluorescein residue of the double-labeled DNA substrate, in the presence of the polymerase, is included in Figure 2b. In the presence of rat pol β, the sensitized fluorescence intensity of the fluorescein residue at the 5′ end of the primer is increased ~3.5-fold. The observed changes in both donor and acceptor emission spectra indicate a large increase of the fluorescence energy transfer as compared to the DNA substrate in the absence of the polymerase.

Analogous fluorescence energy transfer experiments have been performed using different donor−acceptor pairs, or the same donor−acceptor pair, but with interchanged locations on the DNA substrate, depicted in Figure 1. Fluorescence energy transfer parameters for the studied different donor−acceptor pairs and different arrangements of the donor−acceptor pairs are included in Table 1. A characteristic feature of the studied systems is that the fluorescence energy transfer efficiency, E_D, determined using donor emission quenching is often different from the fluorescence energy transfer efficiency, E_A, obtained from the sensitized emission of the acceptor. This is true for measurements performed in the absence and in the presence of the polymerase (Table 1). Such difference between E_D and E_A indicates the presence of some additional nondipolar effects on emission intensities of the fluorescent markers in the examined systems. The true Förster fluorescence transfer efficiency, E_{10}, is then described by eq 6 and is included in Table 1.

As mentioned above (Materials and Methods), there is a significant uncertainty in the distance determination because the factor κ^2 is not directly experimentally accessible (*31*−*33*). On the other hand, if the same spatial separation is examined using a series of different donor−acceptor pairs and interchanging locations, which provides similar distance values using $\kappa^2 = 0.67$, then the lack of any peculiar effect of κ^2 on the distance measurements is established (see Discussion). Nevertheless, we have determined the limiting anisotropies of the donor and acceptor on the DNA substrates to assess mobilities of the donor and acceptor on the time scale of their fluorescence lifetimes by examining their anisotropy decays (*31*, *37*, *38*). This approach is equivalent to the Perrin plot analysis at intermediate values of viscosity where macromolecular rotation is prevailing, without changing the temperature or introducing any additional solute to change the viscosity of the sample (*37*, *38*). Experiments have been performed for all examined DNA substrates, free and in complex with the polymerase (data not shown). The values of all obtained limiting anisotropies are below 0.27; i.e., the limiting anisotropies are significantly lower than fundamental anisotropies, $r_o = 0.4$, of the examined donor and acceptor molecules at the selected excitation wavelengths (Materials and Methods). These results provide additional information that the donor and the acceptor possess significant rotational mobility on the time scale of their fluorescence lifetimes (*37*, *38*). They confirm the results of the multiple donor−acceptor approach, that the determined Förster fluorescence energy transfer efficiency, E, is not strongly affected by any peculiar orientation and immobilization of the donor and acceptor (see Discussion).

The average distances between the donor and acceptor, located at the 5′ end of the template-primer strand, and the acceptor/donor, located at the 5′ end of the primer for the considered DNA substrate (Figure 1), have been calculated using eq 7a and are included in Table 1. It is evident that different donor−acceptor pairs, or the same donor−acceptor pair placed in opposite orientations, provide a similar distance for the determined donor−acceptor spatial separation. The distance between the 5′ ends of the DNA substrates in the absence of rat pol β, averaged over all examined donor−acceptor systems, is $R = 68.1 \pm 2.3$ Å. This distance should be compared to a spatial separation of the 5′ ends of a reference DNA molecule. Such reference is provided by a corresponding dsDNA oligomer in the B-conformation that has a well-defined, rodlike structure in solution (*39*−*41*). Notice that the donor and the acceptor in the considered DNA substrates are located at the opposite 5′ ends of the DNA substrates; i.e., they would be on the same side of the DNA molecule if placed in the completely dsDNA conformation. Moreover, in the examined solution conditions adenine oligomers form helical structure with strong base−base stacking interactions, very similar to the stacking interactions of a single strand within the B-structure of the dsDNA (*39*−*41*). Thus, the reference distance between 5′ ends of DNA substrates, depicted in Figure 1, is the corresponding length of the dsDNA.

The separation between base pairs in the B-structure of the dsDNA is ~3.4 Å (*39*). However, the fluorescein residue, introduced through phosphoramidate, and the CP moiety attached through the six-carbon linker contribute additionally to the length of the DNA substrate that amounts to an extra two bases. Thus, the reference distance between the donor and acceptor in the considered template-primer DNA substrates corresponds to the dsDNA 22-mer and is 74.8 Å. Therefore, the obtained average distance of 68.1 ± 2.3 Å indicates that the ssDNA extension with ten nucleotide residues in length is not protruding from the dsDNA part of the substrate, as a corresponding single strand in the fully dsDNA, but is placed at an angle with respect to the dsDNA conformation, leading to a significantly shorter average spatial separation between the donor and the acceptor (see Discussion).

Fluorescence energy transfer parameters obtained for the template-primer DNA substrates in the complex with rat pol β are included in Table 1. The very pronounced changes in the emission spectra of the donor and the acceptor in the presence of the polymerase (Figure 2) are reflected in the much higher values of the Förster fluorescence energy transfer efficiency, E_{10}, as compared to the free DNA substrates. This is clear evidence that the distance between the donor and acceptor is strongly diminished in the presence of pol β. Because binding of the enzyme to the ssDNA in the (pol β)$_5$ binding mode and to the dsDNA does not induce detectable changes in the fluorescence energy transfer efficiency (data not shown), the observed strong increase of E_{10} must exclusively originate from the formation of the template-primer complex. However, recall that, at the applied enzyme and nucleic acid concentrations (9×10^{-7} and 3×10^{-7} M), the template-primer complex constitutes a fraction of $Q_{TP} = 0.83$ of the total population of the DNA molecules. The remaining fraction of $Q_R = 0.17$ of formed complexes contains the enzyme bound to the ssDNA extension in the (pol β)$_5$ binding mode, or bound to the dsDNA, with the fluorescence energy transfer efficiency, E_R, very similar to the one observed for the free DNA. Therefore, the experimentally observed fluorescence energy transfer efficiency, E_{10}, is related to the fluorescence energy transfer efficiency in the template-primer complex, E_{TP}, by

$$E_{10} = Q_{TP}E_{TP} + (Q_F + Q_R)E_F \qquad (10a)$$

and

$$E_{TP} = \frac{E_{10} - (Q_F + Q_R)E_F}{Q_{TP}} \qquad (10b)$$

The obtained values of the E_{TP} and corresponding distances, R_{TP}, are included in Table 1.

The distance between the donor/acceptor at the 5′ end of the template strand and the donor/acceptor at the 5′ end of the primer, in the presence of rat pol β, averaged over all examined donor−acceptor systems, is $R_{TP} = 58.3 \pm 3$ Å. Comparison with the analogous distance in the free DNA molecule (68.1 ± 2.3 Å) indicates that in the complex with the polymerase the 5′ end of the template strand of the template-primer DNA substrate is closer to the 5′ end of the primer by a distance of 9.8 ± 2.7 Å. On the other hand, the distance between the DNA 5′ ends, in the presence of the polymerase, is 16.5 ± 2.9 Å shorter as compared to the reference distance of 74.8 Å between the 5′ ends of the reference dsDNA 22-mer (see above). Such large distance changes in the DNA molecule bound in the template-primer complex to rat pol β, in solution, strongly indicate that the template-primer DNA is bent in the DNA-binding site of the enzyme to a much larger extent than the free DNA molecule in the absence of the enzyme (see Discussion).

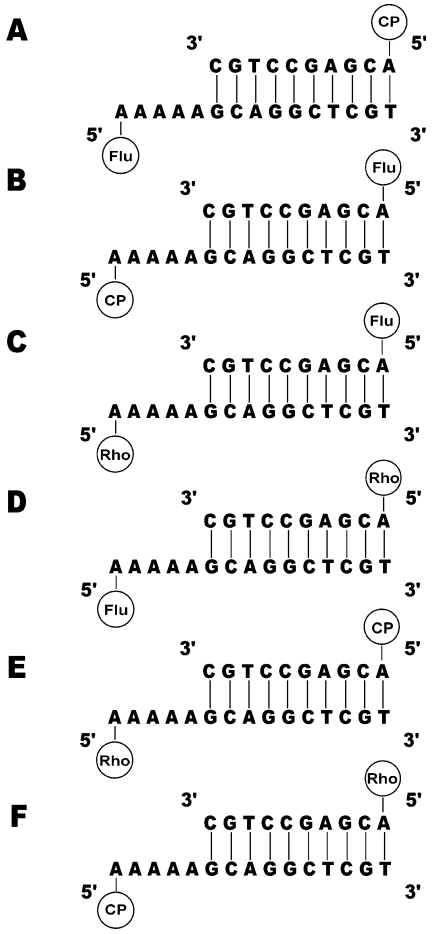

FIGURE 3: Template-primer DNA substrates with ssDNA extension containing five nucleotide residues, used in fluorescence energy transfer experiments to examine the tertiary structure of the template-primer DNA substrates in the template-primer complex with rat pol β. The duplex parts of each substrate, containing the primer oligomer, are ten bps long. The 5′ end of the template strand and the primer are labeled with the fluorescent marker, coumarin (CP), fluorescein (Flu), and rhodamine (Rho), that serves as a donor or acceptor in the fluorescence energy transfer analyses (Materials and Methods). There are six possible arrangements of the selected three donor−acceptor pairs designated as substrates A, B, C, D, E, and F.

Average Distances between the 5′ End of the Template-Primer Strand and the 5′ End of the Primer in the DNA Substrate Having a Five Nucleotide Residue Long ssDNA Extension in the Complex with Rat Pol β. To obtain further insight into the topology of the template-primer DNA−rat pol β complex, we performed fluorescence energy transfer measurements of the distance between the 5′ end of the template strand and the 5′ end of the primer for the DNA molecule having the ssDNA extension with only five nucleotide residues. The DNA substrates used in these studies are depicted in Figure 3.

Binding of rat pol β to the template-primer DNA substrate depicted in Figure 3 is different from the previously

Table 2: Fluorescence Energy Transfer Parameters for Template-Primer DNA Substrates Having Five Nucleotide Residues in the ssDNA Extension in the Absence and Presence of Rat Pol β in Buffer C (pH 7.0, 10 °C) Containing 100 mM NaCl and 1 mM $MgCl_2$[a]

template-primer DNA (Figure 5)	E_D	E_A	E_5	E_{TP}	R[b] (Å)	R_{TP}[b] (Å)
A	0.35 ± 0.01	0.15 ± 0.01	0.19 ± 0.01		66.2 ± 0.8	
B	0.28 ± 0.01	0.24 ± 0.01	0.25 ± 0.01		62.4 ± 0.8	
C	0.40 ± 0.01	0.44 ± 0.01	0.42 ± 0.01		57.0 ± 0.8	
D	0.57 ± 0.01	0.30 ± 0.01	0.41 ± 0.01		57.4 ± 0.8	
E	0.10 ± 0.01	0.21 ± 0.01	0.19 ± 0.01		59.8 ± 0.8	
F	0.21 ± 0.01	0.29 ± 0.01	0.27 ± 0.01		55.5 ± 0.8	
					R_{av}:[c] 59.7 ± 3.6	
A + rat pol β	0.51 ± 0.01	0.23 ± 0.01	0.32 ± 0.01	0.38 ± 0.01		56.4 ± 0.8
B + rat pol β	0.50 ± 0.01	0.28 ± 0.01	0.36 ± 0.01	0.41 ± 0.01		55.3 ± 0.8
C + rat pol β	0.42 ± 0.01	0.47 ± 0.01	0.45 ± 0.01	0.46 ± 0.01		55.5 ± 0.8
D + rat pol β	0.61 ± 0.01	0.33 ± 0.01	0.46 ± 0.01	0.48 ± 0.01		54.7 ± 0.8
E + rat pol β	0.29 ± 0.01	0.46 ± 0.01	0.39 ± 0.01	0.48 ± 0.01		47.6 ± 0.8
F + rat pol β	0.32 ± 0.01	0.44 ± 0.01	0.39 ± 0.01	0.44 ± 0.01		49.0 ± 0.8
						R_{TPav}:[c] 53.1 ± 3.4

[a] Details in the text. [b] The error is the standard deviation obtained from three to four independent experiments. [c] The error is the standard deviation determined using distances for all six DNA substrates.

considered DNA molecule with the ssDNA extension having ten nucleotide residues (Figure 1). The enzyme binds to the DNA forming a template-primer complex; however, it includes the engagement in interactions the ss/dsDNA junction of the substrate and weaker interactions with the short ssDNA extension (*10, 11*). As a result, the affinity of this template-primer complex is lower than the affinity observed for the DNA substrates with a longer ssDNA extension. Independently, another pol β molecule binds to the dsDNA part. At saturation, two polymerase molecules bind to the considered DNA substrate. In the considered case, the partition function of the rat pol β−template-primer DNA system, Z_5, is (*11*)

$$Z_5 = 1 + (K_{TP} + K_{DS})P_F + K_{TP}K_{DS}\,P_F^{\,2} \qquad (11)$$

The fractional molar contributions of the free nucleic acid, Q_F, complexes containing the template-primer complex, Q_{TP}, and without the template-primer complex, Q_R, are

$$Q_F = \frac{1}{Z_5} \qquad (12a)$$

$$Q_{TP} = \frac{K_{TP}P_F + K_{TP}K_{DS}\,P_F^{\,2}}{Z_5} \qquad (12b)$$

and

$$Q_R = \frac{K_{DS}P_F}{Z_5} \qquad (12c)$$

The values of all binding parameters have been obtained in equilibrium fluorescence titration experiments, as described before, which provided $K_{TP} = (4.6 \pm 1) \times 10^6\ M^{-1}$ and $K_{DS} = (1.8 \pm 0.6) \times 10^6\ M^{-1}$ (data not shown) (*11*). At selected concentration of the nucleic acid (3×10^{-7} M) and [rat pol β]$_{total} = 9 \times 10^{-7}$ M, the template-primer complex constitutes Q_{TP}, ~70% of all the nucleic acid species.

Analyses of the obtained fluorescence energy transfer have been performed in an analogous way as described above (Figure 2). The obtained data for all examined template-primer DNA substrates are included in Table 2. In the case of the free DNA molecule, the distance between the donor/acceptor at the 5′ end of the template strand and the donor/acceptor at the 5′ end of the primer, averaged over all examined donor−acceptor systems, is $R = 59.7 \pm 3.6$ Å. Analogously, as we discussed above, for the corresponding reference dsDNA 15-mer, containing ~2.5 turns of the DNA B-structure helix, the opposite 5′ ends are on the same side of the DNA molecule and the distance between them is 51 Å (*39*). Taking into account the contributions of the fluorescein and CP residues, the reference distance between the donor and acceptor in a rodlike structure for the examined DNA substrates corresponds to a dsDNA 17-mer, i.e., 57.8 Å. Therefore, the obtained average distance of 59.7 ± 3.6 Å indicates that, unlike the longer ten nucleotide ssDNA extension, the ssDNA extension with five nucleotide residues in length is protruding from the dsDNA part of the substrate, as a corresponding single strand in the dsDNA. In other words, the ssDNA extension with five nucleotide residues is not long enough to assume the bent conformation in the free template-primer DNA molecule in solution.

Fluorescence energy transfer parameters, E_D, E_A, and E_5, obtained for the template-primer DNA substrates with a five nucleotide residue long ssDNA extension, in the complex with rat pol β, are included in Table 2. As described above, to obtain the fluorescence transfer efficiency characterizing the template-primer complex, one has to take into account the fact that in the applied enzyme and nucleic acid concentrations the template-primer complex constitutes a molar fraction, $Q_{TP} = 0.70$, of the total population of the DNA molecules (see above). The remaining fractions of $Q_F = 0.16$ and $Q_R = 0.14$ correspond to the free DNA and complexes containing the enzyme bound to the dsDNA, with the fluorescence energy transfer efficiency virtually the same as observed for the free DNA (data not shown). Therefore, the experimentally obtained fluorescence energy transfer efficiency, E, determined for the considered DNA substrates is related to the actual fluorescence energy transfer efficiency in the template-primer complex, E_{TP}, by eqs 10a and 10b. The obtained values of the E_{TP} and corresponding distances, R_{TP}, are included in Table 2.

The average distance between the 5′ end of the template strand and the 5′ end of the primer, in the template-primer complex with rat pol β, is $R_{TP} = 53.1 \pm 3.4$ Å as compared to 59.7 ± 3.6 Å in the free DNA molecule (Table 2). Thus,

in the complex, the 5′ end of the template strand of the DNA substrate is at a distance shorter by ~6.6 and ~4.7 Å than in the free DNA and the reference dsDNA, respectively. These data indicate that a significant bend of the DNA molecule in the template-primer complex occurs, even with the DNA substrate having only five nucleotide residues in the ssDNA extension (see Discussion).

Distances between the 5′ Ends of the Gapped DNA Substrate Having a Single Nucleotide Residue in the Gap in the Complex with Rat Pol β. Analogously to the template-primer DNA substrates, we addressed the topology of the gapped DNA−rat pol β complex by measuring distances between the opposite 5′ ends for the gapped DNA molecule having a single nucleotide residue in the gap. The gapped DNA substrates used in these studies are depicted in Figure 4. Interactions of rat pol β with considered gapped DNA substrates have been quantitatively examined before (*10*, *11*). The enzyme−DNA substrate system is described by a set of three independent, different binding sites with the partition function, Z_G, defined as

$$Z_G = 1 + (K_{DS1} + K_{DS2} + K_G)P_F + (K_{DS1}K_{DS2} + K_{DS1}K_G + K_{DS2}K_G)P_F^2 + K_{DS1}K_{DS2}K_G P_F^3 \quad (13)$$

where K_G is the binding constant characterizing the association with the ssDNA gap, i.e., the formation of the gap complex. K_{DS1} and K_{DS2} are the binding constants characterizing the association with the dsDNA downstream from the primer and at the primer location, respectively. At saturation, three polymerase molecules bind to the gap DNA substrate (*10*, *11*). The molar fractional contributions of the free nucleic acid, Q_F, complexes containing gap complex, Q_G, and without gap complex, Q_R, to the total DNA species population are

$$Q_F = \frac{1}{Z_G} \quad (14a)$$

$$Q_G = \frac{K_G P_F + K_G(K_{DS1} + K_{DS2})P_F^2 + K_{DS1}K_{DS2}K_G P_F^3}{Z_G} \quad (14b)$$

and

$$Q_R = \frac{(K_{DS1} + K_{DS2})P_F + K_{DS1}K_{DS2}P_F^2}{Z_G} \quad (14c)$$

Values of all binding parameters have been obtained in equilibrium fluorescence titration experiments which provided $K_G = (2 \pm 1) \times 10^7$ M^{-1}, $K_{DS1} = (2 \pm 0.5) \times 10^6$ M^{-1}, and $K_{DS2} = (2.5 \pm 0.8) \times 10^5$ M^{-1} (*11*). At selected concentration of the nucleic acid (3×10^{-7} M) and [rat pol β]$_{total}$ = 9×10^{-7} M, the DNA species containing the gap complex constitute ~90% of all nucleic acid species.

Fluorescence energy transfer efficiencies, E_D, E_A, E_G, and E_{GP}, obtained for the free gap DNA substrates and in the complex with rat pol β, are included in Table 3. In the case of the free DNA molecule, the distance between the donor and acceptor at the opposite 5′ ends, averaged over all examined donor−acceptor systems, is $R_G = 72.2 \pm 2.6$ Å (Table 3). Because of contributions from the fluorescein, the CP residue, and the single adenosine residue in the gap, the reference distance between the donor and acceptor for the examined gap DNA substrates corresponds to a dsDNA 23-mer, i.e., 78.2 Å (see above). Therefore, similar to the template-primer DNA substrate discussed above, the obtained average distance of 72.2 ± 2.6 Å indicates that, in solution, the free gap DNA, containing a single nucleotide residue in the gap, is significantly bent as compared to the corresponding reference dsDNA oligomer.

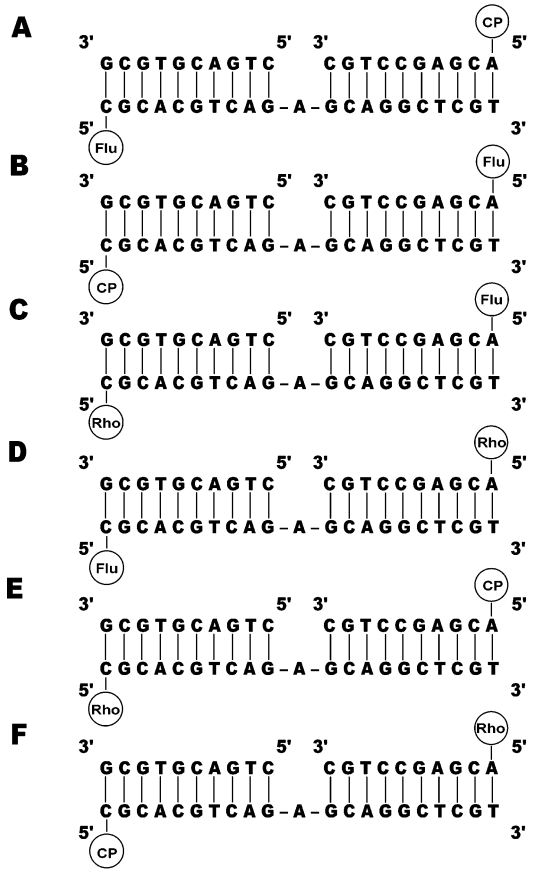

FIGURE 4: Gapped DNA substrates used in fluorescence energy transfer experiments to examine the tertiary structure of the gapped DNA in the gap complex with rat pol β. DNA substrates have two dsDNA parts at the 5′ (downstream from the primer) and 3′ end (primer) of the template strand. The dsDNA parts are identical in all substrates. The dsDNA parts are separated by the ssDNA gap containing one adenine nucleotide residue. The 5′ end of the template strand and the primer are labeled with the fluorescent marker, coumarin (CP), fluorescein (Flu), and rhodamine (Rho), that serves as a donor or acceptor in the fluorescence energy transfer analyses (Materials and Methods). There are six possible arrangements of the selected three donor−acceptor pairs designated as substrates A, B, C, D, E, and F.

In the presence of rat pol β, the gap complex constitutes a fraction of $Q_G = 0.90$ of the total population of the DNA species (see above). The fluorescence energy transfer efficiency in the gap complex, E_{GP}, is related to the experimentally obtained fluorescence energy transfer efficiency, E_G, by the same expressions as in eqs 10a and 10b, with the quantity E_{10} replaced by E_G. The obtained values of the E_{GP} and corresponding distances, R_{GP}, are included in Table 3. The average distance between the 5′ end of the template strand and the 5′ end of the primer, in the template-primer complex with rat pol β, is $R_{GP} = 66 \pm 2.2$ Å (Table 3). Thus, in the gap complex, the distance between the 5′ ends of the DNA is shorter by ~6.2 Å than in the free DNA molecule in solution and ~12.2 Å shorter than the expected

Table 3: Fluorescence Energy Transfer Parameters for Gapped DNA Substrates Having One Nucleotide Residue in the ssDNA Gap in the Absence and Presence of Rat Pol β in Buffer C (pH 7.0, 10 °C) Containing 100 mM NaCl and 1 mM $MgCl_2$[a]

gapped DNA (Figure 6)	E_D	E_A	E_G	E_{GP}	R_G[b] (Å)	R_{GP}[b] (Å)
A	0.04 ± 0.01	0.12 ± 0.01	0.11 ± 0.01		73.7 ± 1.2	
B	0.08 ± 0.01	0.12 ± 0.01	0.12 ± 0.01		72.5 ± 1.2	
C	0.22 ± 0.01	0.14 ± 0.01	0.15 ± 0.01		72.1 ± 1.2	
D	0.12 ± 0.01	0.11 ± 0.01	0.11 ± 0.01		76.5 ± 1.5	
E	0.04 ± 0.01	0.10 ± 0.01	0.09 ± 0.01		69.1 ± 1.2	
F	0.05 ± 0.01	0.10 ± 0.01	0.09 ± 0.01		69.1 ± 1.2	
					R_{Gav}:[c] 72.2 ± 2.6	
A + rat pol β	0.11 ± 0.01	0.17 ± 0.01	0.16 ± 0.01	0.17 ± 0.01		67.7 ± 1
B + rat pol β	0.09 ± 0.01	0.17 ± 0.01	0.16 ± 0.01	0.16 ± 0.01		68.6 ± 1
C + rat pol β	0.24 ± 0.01	0.24 ± 0.01	0.24 ± 0.01	0.25 ± 0.01		64.9 ± 1
D + rat pol β	0.14 ± 0.01	0.24 ± 0.01	0.23 ± 0.01	0.23 ± 0.01		67.3 ± 1
E + rat pol β	0.07 ± 0.01	0.13 ± 0.01	0.12 ± 0.01	0.12 ± 0.01		65.5 ± 1
F + rat pol β	0.12 ± 0.01	0.15 ± 0.01	0.15 ± 0.01	0.16 ± 0.01		62.0 ± 1
						R_{GPav}:[c] 66.0 ± 2.2

[a] Details in the text. [b] The error is the standard deviation obtained from three to four independent experiments. [c] The error is the standard deviation determined using distances for all six DNA substrates.

full length of ~78.2 Å of the corresponding dsDNA 23-mer (see Discussion).

Distances between the 5′ Ends of the Gapped DNA Substrate with a Single Nucleotide Residue in the Gap and a 5′-Terminal Phosphate Group in the Complex with Rat Pol β. The 5′-terminal phosphate group in the gapped DNA is a common intermediate product in the base excision repair process (*6*). Therefore, we also addressed the topology of the rat pol β complex with the gapped DNA containing the 5′-terminal phosphate group. The gapped DNA substrates used in these studies are depicted in Figure 5. The enzyme−DNA substrate systems are described by the same partition function and the same molar fractional contributions of different DNA−polymerase species, as applied to analogous gapped DNA substrates without the phosphate group. They are defined by eqs 14 and 15. The values of the corresponding binding constants are $K_G = (6 \pm 1) \times 10^7$ M^{-1}, $K_{DS1} = (2 \pm 0.5) \times 10^6$ M^{-1}, and $K_{DS2} = (2.3 \pm 0.8) \times 10^5$ M^{-1} (*11*). Because of the higher value of K_G, at the selected concentration of the nucleic acid (3×10^{-7} M) and [rat pol $\beta]_{total} = 9 \times 10^{-7}$ M, the DNA species containing the gap complex constitutes ~96% of all nucleic acid species. Fluorescence energy transfer efficiencies, E_D, E_A, E_G, and E_{GP}, obtained for the free gap DNA substrates and in the complex with rat pol β, are included in Table 4.

In the case of the free DNA molecule, the distance between the donor/acceptor at the opposite 5′ ends, averaged over all examined donor−acceptor systems, is $R_G = 70.9 \pm 3.1$ Å (Table 4). This distance is very similar to the one obtained for the gapped DNA substrate without the phosphate group and indicates that the DNA molecule is significantly bent as compared to the corresponding dsDNA 23-mer with the length of 78.2 Å. In other words, the free gapped DNA substrate with the 5′-terminal phosphate group is significantly bent, even in the absence of the enzyme, to the same extent as the substrate without the phosphate group discussed above. In the presence of rat pol β, the average distance between the 5′ ends in the gap complex is additionally shortened to $R_{GP} = 65.5 \pm 3.1$ Å (Table 4).

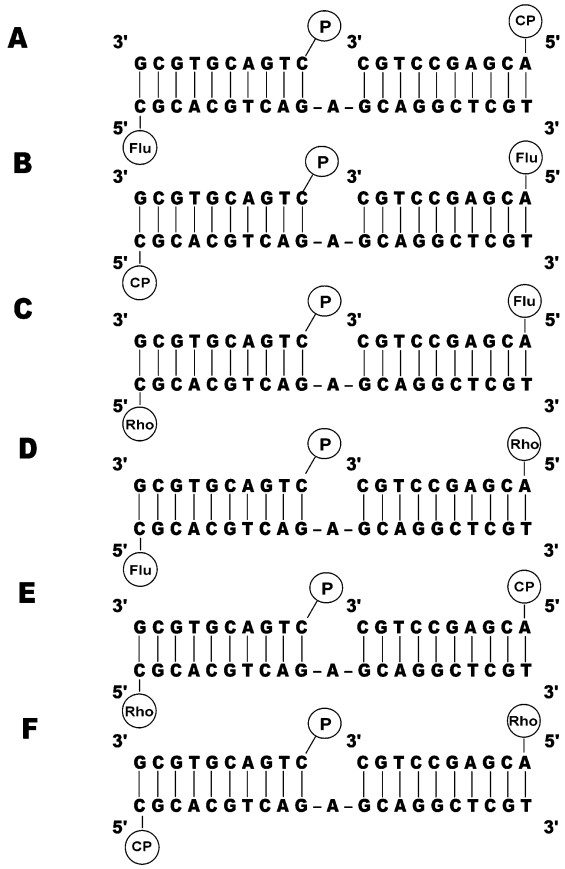

FIGURE 5: Gapped DNA substrates that contain one adenine nucleotide in the ssDNA gap and the 5′-terminal phosphate group downstream from the primer, used in fluorescence energy transfer experiments to examine the tertiary structure of the gapped DNA in the complex with rat pol β. The DNA substrates have two dsDNA parts at the 5′ (downstream from the primer) and 3′ end (primer) of the template strand. The dsDNA parts are identical in all DNAs. The dsDNA parts are separated by the ssDNA gap containing one adenine nucleotide residue. The 5′ end of the template strand and the primer are labeled with the fluorescent marker, coumarin (CP), fluorescein (Flu), and rhodamine (Rho), that serves as a donor or acceptor in the fluorescence energy transfer analyses (Materials and Methods). Six possible arrangements of the selected three donor−acceptor pairs are designated as substrates A, B, C, D, E, and F.

DISCUSSION

A crucial insight into the structure of the macromolecular complexes can be directly accessed through the distance measurements between the different parts of the examined complexes (*31*, *32*, *40*−*44*). The fluorescence energy transfer

Table 4: Fluorescence Energy Transfer Parameters for Gapped DNA Substrates Having One Nucleotide Residue in the ssDNA Gap and a 5′-Terminal Phosphate Group Downstream from the Primer in the Absence and Presence of Rat Pol β in Buffer C (pH 7.0, 10 °C) Containing 100 mM NaCl and 1 mM $MgCl_2$[a]

gapped DNA 5′-terminal PO_4^- (Figure 8)	E_D	E_A	E_G	E_{GP}	R_G[b] (Å)	R_{GP}[b] (Å)
A	0.05 ± 0.01	0.13 ± 0.01	0.11 ± 0.01		72.5 ± 1.2	
B	0.10 ± 0.01	0.12 ± 0.01	0.12 ± 0.01		72.5 ± 1.2	
C	0.11 ± 0.01	0.14 ± 0.01	0.14 ± 0.01		73.1 ± 1.2	
D	0.06 ± 0.01	0.14 ± 0.01	0.13 ± 0.01		74.1 ± 1.2	
E	0.09 ± 0.01	0.12 ± 0.01	0.11 ± 0.01		66.6 ± 1	
F	0.16 ± 0.01	0.10 ± 0.01	0.11 ± 0.01		66.6 ± 1	
					R_{Gav}:[c] 70.9 ± 3.1	
A + rat pol β	0.11 ± 0.01	0.22 ± 0.01	0.20 ± 0.01	0.20 ± 0.01		65.5 ± 1
B + rat pol β	0.14 ± 0.01	0.20 ± 0.01	0.19 ± 0.01	0.19 ± 0.01		66.2 ± 1
C + rat pol β	0.15 ± 0.01	0.19 ± 0.01	0.18 ± 0.01	0.18 ± 0.01		69.5 ± 1
D + rat pol β	0.04 ± 0.01	0.15 ± 0.01	0.18 ± 0.01	0.18 ± 0.01		69.5 ± 1
E + rat pol β	0.19 ± 0.01	0.15 ± 0.01	0.16 ± 0.01	0.16 ± 0.01		62.0 ± 1
F + rat pol β	0.11 ± 0.01	0.20 ± 0.01	0.18 ± 0.01	0.18 ± 0.01		60.5 ± 1
						R_{GPav}:[c] 65.5 ± 3.1

[a] Details in the text. [b] The error is the standard deviation obtained from three to four independent experiments. [c] The error is the standard deviation determined using distances for all six DNA substrates.

method is the most often used approach in accessing macromolecular structures in solution (*31*, *37*, *38*, *42*−*45*). This "spectroscopic ruler" is particularly useful in determining distances in large macromolecular systems in solution that are unavailable by any other methods. The method has been extensively and successfully used in examination nucleic acid structure including DNA polymerase−DNA complexes (*46*−*49*). However, the strength of the method is weakened by the orientation tensor, κ^2, although only extreme values of $\kappa^2 \approx 0$ or ≈ 4 can strongly affect the measured distance. Several analyses indicate that the difference in distance determination is mostly in the range of ±10% from the distances obtained with the assumed value of $\kappa^2 = 0.67$, i.e., with the assumed complete randomizations of the donor and acceptor dipole orientation (*42*, *43*). The major weakness results from the fact that the parameter, κ^2, cannot be experimentally determined. The available analyses allow the experimenter to determine only the range of probable distances that is usually too large to be useful in evaluations of subtle conformational changes in macromolecular systems (*33*).

However, as we pointed out, the estimate of the κ^2 effect on the determined distance is exclusively based on the rigorous analysis of a *single* donor−acceptor pair and a *single* set of their locations (*33*). In this context, the multiple configuration, multiple donor−acceptor approach, applied by us, provides an *empirical* test of the effect of κ^2 on the determined distance. The approach is based on the fact that different fluorescence donors and acceptors, with similar R_o, have different structures that have different orientations of absorption and emission dipoles, respectively, when placed on the examined macromolecular system (*24*, *25*). This provides the required randomness of the dipole orientations necessary to quantitatively evaluate the distances. Additional randomization of the dipole orientations is achieved by interchanging the donor and acceptor in their locations on the macromolecule. This is particularly easy to experimentally realize in the case of nucleic acid oligomers because of the technological advancement in labeling techniques that allow the experimenter to place various donors or acceptors in practically any location on the molecule. Measurements of the same spatial separation, using different donor−acceptor pairs and interchanging their locations, that give very similar values of the donor−acceptor distance using $\kappa^2 = 0.67$, provide the required empirical evidence that none of the examined donor−acceptor system is affected by extreme values of κ^2. The measured distance, when averaged over all examined donor−acceptor systems, reflects then the true spatial separation of the donor and the acceptor in the examined macromolecular system (Tables 1−4) (*24*).

Binding of rat pol β to the template-primer DNA substrate with the ssDNA extension having ten nucleotide residues is a complex process that includes the formation of the $(\text{pol } \beta)_5$ binding mode, template-primer complex, and binding of the enzyme to the dsDNA part of the DNA molecule (*11*). In the template-primer complex the enzyme engages both the ssDNA of the template strand and the dsDNA part of the DNA molecule. The 3′ end of the primer is placed in the active site of the polymerase; i.e., this is the functional configuration in the DNA synthesis. Similar template-primer complex is formed with the DNA substrates having only five nucleotide residues in the ssDNA extension, however, with lower affinity due to the weaker engagement of the 8 kDa domain of the enzyme in interactions with the template strand (*11*). In both cases, the template-primer configuration dominates the enzyme binding to the DNA substrate only in a narrow range of the enzyme concentration (*11*). Thus, knowledge of all intrinsic interaction parameters is crucial for the extraction of fractional molar contributions of all complexes containing the template-primer configuration from other complexes.

The Template Strand of the Template-Primer DNA Substrate in the Complex with Pol β Is Bent between the Third and Fourth Nucleotide in the ssDNA Extension at the Angle 85 ± 7° with Respect to the dsDNA Part of the DNA Substrate, Independently of the Length of the ssDNA Extension. The available resolution of the crystal structure of the template-primer DNA−polymerase complex does not allow a rigorous determination of the conformation of the template-primer DNA (*7*, *50*). Moreover, difference in environments between crystallization conditions and solution studies poses a natural and fundamental question to what extent such

conformation occurs in solution. Consideration of the topology of the template-primer DNA molecule in the binding site of rat pol β in solution is facilitated by the fact that we know general aspects of the structure of the involved nucleic acids (Figures 1 and 3), energetics of the protein binding, and formation of kinetic intermediates in the binding process (*8*−*11*, *18*−*21*).

The template-primer DNA molecule is built of two parts, the ssDNA extension and the dsDNA part of equal length. Both parts differ strongly in their flexibility or stiffness. While the persistence length of the dsDNA is ∼150 bps, the same quantity is only ∼15−25 nucleotide residues long in the case of the ssDNA (*40*). Such large difference in the persistence lengths makes models that include direct bending of the dsDNA part of the template-primer DNA molecule very unlikely. Both thermodynamic and kinetic data indicate the lack of any intermediate that would require large enough positive energy input to induce the dsDNA bending with only ten base pairs in length (*8*−*11*, *18*, *20)*. Moreover, the part of crystal structure of the enzyme co-complexes with the dsDNA part of the template-primer substrate, which can be resolved, indicates that the global tertiary structure of the dsDNA part is not affected in the complex, indicating that the bend occurs in the ssDNA part of the DNA substrates (*50*) (see below).

The major parameter describing the topology of the template-primer DNA molecule in the binding site of rat pol β in solution is the angle, Θ_{TP}, at which the DNA molecule is bent, defined as the angle between the tangents to the ends of the DNA molecule, as schematically depicted in Figure 6a (*51*). In the simplest model, the conformational change of the considered DNA results from a single bend of the ssDNA extension. A smooth curvature of the nucleic acid molecule, although it cannot be excluded, is much less probable because of structural features discussed above. However, in general, the single bending can occur at an arbitrary point in the extension. Also, the analysis depends on the length of the ssDNA extension (see below). In the context of the experimentally determined parameter, R_{TP}, the geometry of the model, as applied to the template-primer DNA substrates with ten and five nucleotide residues in the ssDNA extension, is depicted in Figure 6b. Notice that the experimentally determined distance, R_{TP}, is independent of the initial conformation of the free DNA substrate in solution. In other words, it is an *intrinsic property* of the given template-primer−rat pol β complex. On the other hand, the derived analytical relationships should be independent of any specific conformation, adopted by the free DNA substrate in solution, prior to enzyme binding.

As discussed above, this can be achieved if distances between the 5′ ends of the DNA substrates, free in solution and in the complex with the enzyme, are related to the reference length of the examined DNA molecule. Such reference length is provided by comparison with the known length of the corresponding dsDNA in solution that can be approximated by a straight rod with ∼3.4 Å separations between the base pairs (*39*−*41*). For the examined template-primer DNAs, with ten and five nucleotide residues in the ssDNA extension with included donor and acceptor contributions, these corresponding reference lengths are $R_{R10} = 74.8$ Å and $R_{R5} = 57.8$ Å, respectively. Using the diagrams in Figure 6b the value of the bend angle of the considered DNA

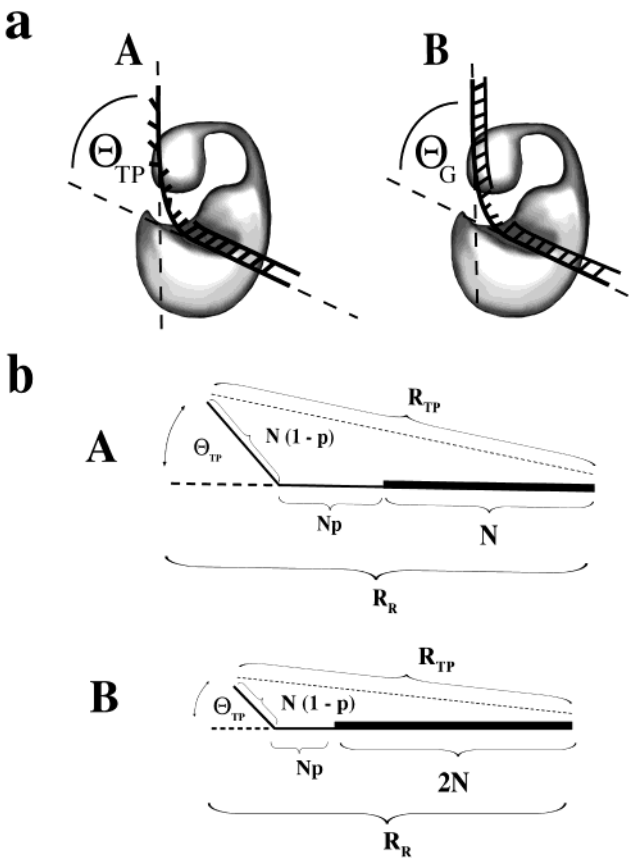

FIGURE 6: (a) Schematic diagrams that show the bend angles, Θ_{TP} and Θ_G, for the tertiary structure of the template-primer DNA (A) and gapped DNA (B) substrates bound in the total DNA-binding site of rat pol β in the template-primer and gap complex, respectively. The bend angles are defined as the angle between the tangents to the ends of the DNA molecule parallel to the axes of the template strand (A) or dsDNA parts of the gapped DNA substrate. (b) The simplest geometric model of the conformational change of the template-primer DNA (A) with the ten bp long dsDNA part and ten nucleotide residues in the ssDNA extension, where the conformational change of the nucleic acid results from a single bend of the ssDNA extension. The bending can occur at an arbitrary point in the ssDNA extension defined by the fractional bending parameter, p. The total length of the DNA, R_R, molecule refers to a corresponding, reference rodlike structure of the dsDNA conformation. In this model the bending angle, Θ_{TP}, is the angle between the axes of the two parts of the molecule. Analogous geometric model for the conformational change of the template-primer DNA with five nucleotide residues in the ssDNA extension (B) and the ten bp long dsDNA part, where the conformational change of the nucleic acid results from a single bend of the ssDNA extension.

substrates can analytically be defined in terms of the experimentally determined R_{TP10} and R_{TP5} and the parameter, p, which we term the fractional bending point. It is a quantity that defines the fraction of the ssDNA extension where the bend occurs; i.e., p assumes values from 0 to 1, although the physical range of p depends on the specific ratio R_{TPN}/R_{RN}, where N is the total length of the ssDNA extension in nucleotides.

For the geometry of the template-primer substrate with ten nucleotide residues in the ssDNA extension, depicted in Figure 6b, the bend angle, Θ_{10}, is then defined as

$$\Theta_{10} = \arccos\left[\left(\frac{2}{1-p^2}\right)\left(\frac{R_{TP10}}{R_{R10}}\right)^2 - \frac{1+p^2}{1-p^2}\right] \quad (15)$$

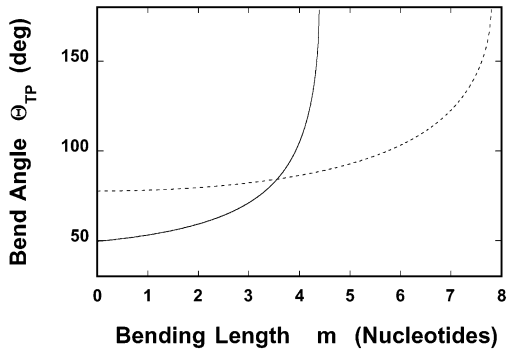

FIGURE 7: Dependence of the bend angle, Θ_{TP}, upon the bending length, *m*, for the template-primer DNA with ten nucleotide residues in the ssDNA extension and the ten bp long dsDNA part (---) and the template-primer DNA with five nucleotide residues in the ssDNA extension, and the ten bp long dsDNA part (—). The plots were generated using eqs 15 and 16, with $R_{R10} = 74.8$ Å, $R_{TP10} = 58.3$ Å (eq 15) and $R_{R5} = 57.8$ Å, $R_{TP5} = 53.2$ Å (eq 16).

In the case of the DNA substrate with five nucleotide residues in the ssDNA extension, the bend angle, Θ_5, is

$$\Theta_5 = \arccos\left[\left(\frac{9}{2(1-p)(2+p)}\right)\left(\frac{R_{TP5}}{R_{R5}}\right)^2 - \frac{1-p}{2(2+p)} - \frac{2+p}{2(1-p)}\right] \quad (16)$$

The length of the ssDNA extension, *m*, where the bend occurs, i.e., the bending length, is related to *p* as $m = Np$.

Figure 7 shows the dependence of the bend angles Θ_{10} and Θ_5 upon the value of *m* for the two specific values of R_{TP10}/R_{R10} and R_{TP5}/R_{R5}, using the experimentally determined R_{TP10} and R_{TP5}. There are two fundamental aspects of these data. First, the smallest angle at which the template-primer ssDNA extension can be bent in the total DNA-binding site of pol β is ~78° and ~51°, i.e., different for the ssDNA extension with ten and five nucleotide residues. It corresponds to the bending point characterized by $m = p = 0$, i.e., at the ss/dsDNA junction for both DNA substrates. Second, it is clear that a multitude of bending points and bend angles of the ssDNA extension in both DNA substrates is compatible with the fluorescence energy transfer data. However, in such cases, the bending would have to occur at very different points on the longer ssDNA than on the shorter ssDNA extension, or the formation of the complex would have to induce different bend angles in both substrates. This would imply that the structure of the total DNA-binding site of the polymerase is very different, depending on the length of the ssDNA extension of the template-primer DNA substrate. This is not indicated by experimental data.

Kinetic studies clearly showed the same conformational transitions, i.e., the same structural changes on the protein−ssDNA complexes upon complex formation, independently of the length of the ssDNA (*18*−*21*). Thus, differences in energetics of the formed intermediates result from limited interactions within the binding site, not from the different topological structures of the binding site. In other words, the data indicate that the template-primer DNA substrates assume the same global conformational state when bound in the template-primer complex, independently of the length of the ssDNA extension, i.e., characterized by the same bend angle, Θ_{TP}, and bending length, *m*. Notice that the plots in Figure 7 show the existence of a bend angle and bending length that are the same for both DNA substrates. The same Θ_{TP} occurs when the bending of the DNA substrate takes place between the third and the fourth nucleotide of the template strand, corresponding to $\Theta_{10} = \Theta_5 = 85 \pm 7°$. Therefore, fluorescence energy transfer data indicate that, in the template-primer complex, the DNA substrate is bent between the third and the fourth nucleotide of the template strand with the ssDNA extension at the angle $\Theta_{TP} = 85 \pm 7°$ with respect to the dsDNA part of the template-primer DNA substrate (Figure 7).

It may seem surprising that the DNA substrate with only five nucleotides in the ssDNA extension assumes the same bend angle as the longer substrate. However, as mentioned above, this would simply mean that once the enzyme associates with the template-primer DNA, the protein assumes a similar conformation in the complex (*8*−*11*, *18*−*21*). Such conformation predominantly is induced by protein−nucleic acid interactions and interplay between both DNA-binding subsites engaged in the complex and less by relative affinities. Thus, similar enzyme conformation occurs in the formation of the (pol β)$_{16}$ binding mode and the template-primer complex, as well as the gap complex, although their affinities are different (*8*−*11*). In other words, the structure of the total DNA-binding site of the protein in a different complex imposes the similar tertiary structure, i.e., the same bend angle for the bound template-primer DNA substrates, independently of the length of the ssDNA extension. Notice that the conformation of the free template-primer DNA substrate with the ssDNA extension having ten nucleotide residues is different from the rodlike conformation of the corresponding dsDNA oligomer and assumes a bent structure in solution, even in the absence of the enzyme. It is very probable that the higher affinity of this DNA substrate for the enzyme results partially from the fact the DNA substrate with ten nucleotide residues in the ssDNA extension is already in a conformation favoring the template-primer complex, as also suggested by the thermodynamic and kinetic studies (*8*−*11*, *18*−*21*).

In the Absence of the 5′-Terminal Phosphate Group, the Gapped DNA Substrate in the Gap Complex with Pol β in Solution Is Bent at the Angle 65 ± 6°, Similar to the Bend Angle Observed in the Crystal Structure of the Enzyme−*DNA Co-complexes*. As found for the template-primer DNA substrate with ten nucleotide residues in the ssDNA extension (see above), the average conformation of the free gapped DNA is different from the corresponding rodlike dsDNA oligomer, before it enters the complex with the polymerase. Because the bending of the gapped DNA must be localized in the ssDNA gap, i.e., in the middle of the DNA molecule, one can estimate the average bend angle, Θ_G, of the gapped DNA in the absence of the enzyme, using $p = 0$. For this value of *p*, eq 15 reduces to

$$\Theta_G = \arccos\left[2\left(\frac{R_G}{R_{RG}}\right)^2 - 1\right] \quad (17)$$

Introducing $R_G = 72.2 \pm 2.6$ Å and $R_{RG} = 78.2$ Å provides $\Theta_G = 45 \pm 8°$. Therefore, the average conformation of the free gapped DNA substrate in solution can be characterized by an average bend angle of ~45°. Formation of the gap complex induces further conformational change in the DNA

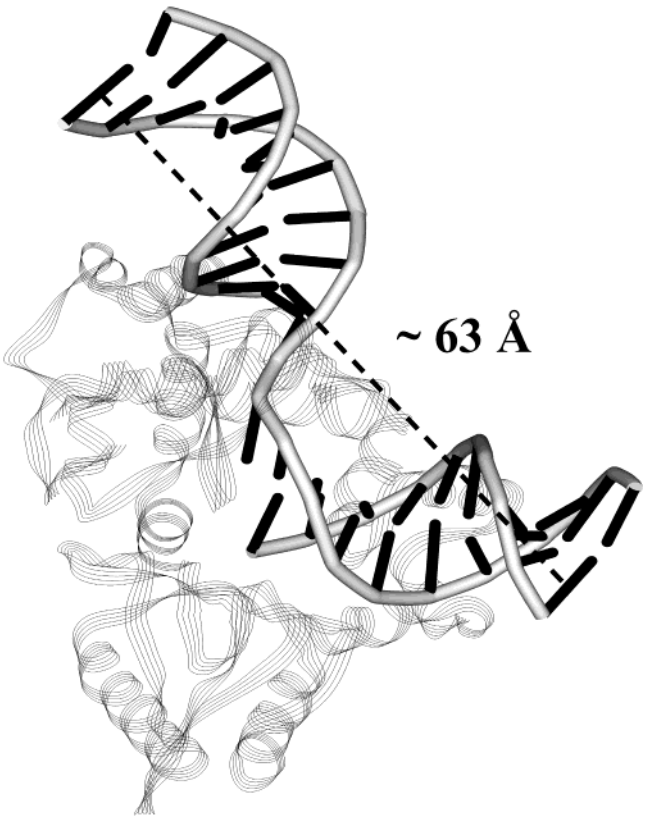

FIGURE 8: Model of the tertiary structure of the gapped DNA, analogous the DNA substrate analyzed in this work, having two ten bp long dsDNA parts (Figure 6) and one nucleotide residue in the gap of the pol β−gapped DNA complex, based on the crystal structure of the human pol β−DNA substrate co-complex (*7*). The structure has been generated using data from Brookhaven Protein Data Bank, under the code 1BPY, using ViewerPro (San Diego, CA). The dashed line is the distance (Å) between the bases at the 5′ end of the template strand and the 5′ end of the primer oligomer (see text for details).

as shown by a decreased distance between the 5′ ends of the DNA substrate to $R_G = 66 \pm 2.2$ Å. Introducing this value to eq 17 provides $\Theta_{GP} = 65 \pm 6°$. This angle is lower by ~20° than $\Theta_{TP} \approx 85°$ obtained for the template-primer complex. However, unlike in the case of the template-primer complex, the template strand of the gapped DNA is not directly involved in interactions with the polymerase in the gap complex (*7*). The enzyme engages the oligomer complementary to the template strand, downstream from the primer, separated from the template strand by a distance of ~20 Å in the dsDNA structure (Figure 6a). As a result, the angle between the tangents to the ends of the gapped DNA in the gap complex, Θ_{GP}, differs from Θ_{TP}, which characterizes the template-primer complex (see below).

Because the crystal structure of the gapped DNA, with one nucleotide in the gap, in the co-complex with the analogous human pol β is available, we can directly compare the obtained distance between the 5′ ends of the gapped DNA in the gap complex and the corresponding bend angle, Θ_{GP}. The model of the pol β co-complex with the gapped DNA analogous to the DNA used in this work, obtained on the basis of the crystal structure, is shown in Figure 8 (*7*). The distance between the bases at two ends of the DNA molecule is 63.2 Å. Taking into account the contributions of the donor and acceptor, which amounts to an additional base pair in each of the dsDNA parts (see above), the expected distance is ~70 Å. This value is in good agreement with the experimentally determined average distance using the multiple donor−acceptor approach, $R_{GP} = 66 \pm 3$ Å. Recall that the bend angle, Θ_{GP}, is defined as the angle between the axes parallel to the axes of the dsDNA parts of the gapped DNA substrate and tangent to the ends of the DNA molecule (Figure 8). The model in Figure 8 indicates that $\Theta_{GP} \approx 60°$. Therefore, the tertiary structure of the gapped DNA, without the 5′-terminal PO_4^- group, in the gap complex with pol β in solution, as characterized by the distance, R_{GP}, and the bend angle, Θ_{GP}, is virtually the same as the tertiary structure of the corresponding crystal structure of the co-complex.

The 5′-Terminal Phosphate Group Does Not Affect the Tertiary Conformation of the Gapped DNA Substrate with Pol β in Solution. The crystal structure of the gap complex with the gapped DNA containing the 5′-terminal phosphate group downstream from the primer is not available. As we mentioned above, the 5′-terminal phosphate group is a common intermediate in the base excision processes (*6*). Thermodynamic data clearly show that the 5′-terminal PO_4^- group does not significantly contribute to the energetics of the enzyme binding to the gap (*10*, *11*). Also, kinetic studies indicate that the phosphate group does not constitute a recognition element for the polymerase, in the initial stage of the gapped DNA substrate recognition, both for rat and for human pol β (*20*, *21*). The determined average distance between the 5′ ends of the bound gapped DNA containing the PO_4^- group and the bend angle are $R_{GP} = 65.5 \pm 3.1$ Å and $\Theta_{GP} = 66.3 \pm 7.7°$; i.e., they are, within experimental accuracy, the same as obtained for the gapped DNA without the PO_4^- group. In other words, the obtained results indicate that the presence of the PO_4^- group does not affect the tertiary structure of the gapped DNA bound to the polymerase in the gap complex.

In this context, it should be pointed out that spectroscopic data, obtained both in equilibrium and in kinetic studies, indicate that the structure of the ssDNA gap is different in the gap complex in the presence of the PO_4^- group (*10*, *11*, *20*, *21*). The bases of the ssDNA gap are significantly more immobilized and separated at a larger distance from each other than in the absence of the phosphate group. However, the energetics and dynamics of the formed complex and intermediates are little affected. These data provide the first indication that the effect of the phosphate group on the structure of the gap complex is localized at the ssDNA gap and is not manifested in the global tertiary structure of the DNA substrate in the complex. Therefore, fluorescence energy transfer results discussed in this work, indicating very similar tertiary structures of the gapped DNA in the gap complex, in the presence and absence of the 5′-terminal phosphate group, corroborate very well with the spectroscopic analyses of the equilibrium and kinetic intermediates in the recognition process of the gapped DNA by pol β.

ACKNOWLEDGMENT

We thank Betty Sordahl for help in preparing the manuscript.

REFERENCES

1. Hubscher, U., Maga, G., and Spadari, S. (2002) *Annu. Rev. Biochem. 71*, 133−163.

2. Friedberg, E. C., Walker, G. C., and Siede, W. (1995) in *DNA Repair and Mutagenesis*, pp 317−365, ASM Press, Washington, DC.
3. Fry, M., and Loeb, L. A. (1986) in *Animal Cell DNA Polymerases*, pp 75−183, CRC Press, Boca Raton, FL.
4. Budd, M. E., and Campbell, J. L. (1997) *Mutat. Res. 384*, 157−167.
5. Hubscher, U., Nasheuer, H.-P., and Syvaoja, J. E. (2000) *Trends Biochem. Sci. 25*, 143−147.
6. Masumoto, Y., and Kim, K. (1995) *Science* 269, 699−702.
7. Pelletier, H., Sawaya, M. R., Wolfle, W., Wilson, S. H., and Kraut, J. (1996) *Biochemistry 35*, 12762−12777.
8. Rajendran, S., Jezewska, M. J., and Bujalowski, W. (1998) *J. Biol. Chem. 273*, 31021−31031.
9. Jezewska, M. J., Rajendran, S., and Bujalowski, W. (1998) *J. Mol. Biol. 284*, 1113−1131.
10. Rajendran, S., Jezewska, M. J., and Bujalowski, W. (2001) *J. Mol. Biol. 308*, 477−500.
11. Jezewska, M. J., Rajendran, S., and Bujalowski, W. (2001) *J. Biol. Chem. 276*, 16123−16136.
12. Nagasawa, K.-I., Kitamura, K., Yasui, A., Nimura, Y., Ikeda, K., Hirai, M., Matsukage, A., and Nakanishi, M. (2000) *J. Biol. Chem. 275*, 31233−31238.
13. Dominguez, O., Ruiz, J. F., Lain de Lera, T., Garcia-Diaz, M., Gonzalez, M. A., Kirchhoff, T., Martinez, A. C., Bernad, A., and Blanco, L. (2000) *EMBO J. 19*, 1731−1742.
14. Garcia-Diaz, M., Dominguez, O., Lopez-Fernandez, L. A., Lain de Lera, T., Saniger, M. L., Ruiz, J. F., Parraga, M., Gacia-Ortiz, M. J., Kirchhoff, T., del Mazo, J., Bernad, A., and Blanco, L. (2000) *J. Mol. Biol. 301*, 851−867.
15. Oliveros, M., Yanez, R. J., Salas, M. L., Vinuela, E., and Blanco, L. (1997) *J. Biol. Chem. 272*, 30899−30910.
16. Jezewska, M. J., Rajendran, S., and Bujalowski, W. (2001) *Biochemistry 40*, 3295−3307.
17. Matsumoto, Y., Kim, K., Katz, D. S., and Feng, J.-A. (1998) *Biochemistry 37*, 6456−6464.
18. Jezewska, M. J., Rajendran, S., Galletto, R., and Bujalowski, W. (2001) *J. Mol. Biol. 313*, 977−1002.
19. Rajendran, S., Jezewska, M. J., and Bujalowski, W. (2001) *Biochemistry 40*, 11794−11810.
20. Jezewska, M. J., Galletto, R., and Bujalowski, W. (2002) *J. Biol. Chem. 277*, 20316−20327.
21. Jezewska, M. J., Galletto, R., and Bujalowski, W. (2003) *Mol. Cell. Biophys. Biochem.* (in press).
22. Jezewska, M. J., Rajendran, S., and Bujalowski, W. (1998) *Biochemistry 37*, 3116−3136.
23. Jezewska, M. J., Rajendran S., and Bujalowski, W. (1998) *J. Biol. Chem. 273*, 9058−9069.
24. Jezewska, M. J., Rajendran S., Bujalowska, D., and Bujalowski, W. (1998) *J. Biol. Chem. 273*, 10515−10529.
25. Jezewska, M. J., and Bujalowski, W. (1996). *Biochemistry 35*, 2117−2128.
26. Bujalowski, W., and Klonowska, M. M. (1993) *Biochemistry 32*, 5888−5900.
27. Edeldoch, H. (1967) *Biochemistry 6*, 1948−1954.
28. Gill, S. C., and von Hippel, P. H. (1989) *Anal. Biochem. 182*, 319−326.
29. Bujalowski W., and Jezewska, M. J. (2000) in *Spectrophotometry and Spectrofluorimetry. A Practical Approach* (Gore, M. G., Ed.) pp 141−165, Oxford University Press, Cambridge.
30. Azumi, T., and McGlynn, S. P. (1962) *J. Chem. Phys. 37*, 2413−2420.
31. Lakowicz, J. R. (1999) in *Principle of Fluorescence Spectroscopy*, pp 367−443, Plenum Press, New York.
32. Berman, H. A., Yguerabide, J., and Taylor, P. (1980) *Biochemistry 19*, 2226−2235.
33. Dale, R. E., Esinger, J., and Blumberg, W. E. (1979) *Biophys. J. 26*, 161−194.
34. Parker, C. A., and Reese, W. T. (1960) *Analyst 85*, 587−592.
35. Parker, C. A. (1962) *Anal. Chem. 34*, 502−505.
36. Scott, T. G., Spencer, R. D., Leonard, N. J., and Weber, G. (1970) *J. Am. Chem. Soc. 92*, 687−695.
37. Cantor, C. R., and Schimmel, P. R. (1980) in *Biophysical Chemistry*, Part II, pp 433−466, W. H. Freeman, New York.
38. Fairclough, R. H., and Cantor, C. R. (1978) *Methods Enzymol. 48*, 347−379.
39. Saenger, W. (1984) *Principles of Nucleic Acid Structure*, Springer-Verlag, New York.
40. Bloomfield, V. A., Crothers, D. M., and Tinoco, I. (2000) in *Nucleic Acids. Structure, Properties, and Functions*, pp 414−433, University Science Books, Sausalito, CA.
41. Mandelkern, M., Elias, J. G., Eden, D., and Crothers, D. M. (1981) *J. Mol. Biol. 155*, 153−161.
42. Stryer, L. (1978) *Annu. Rev. Biochem. 47*, 819−846.
43. Hass, E., Katchalski-Katzir, E., and Stenberg, I. Z. (1978) *Biochemistry 17*, 5064−5070.
44. Cheung, H. C., Wang, C.-K., and Garland, F. (1982) *Biochemistry 21*, 5135−5142.
45. Cantor, C. R., and Pechukas, P. (1971) *Proc. Natl. Acad. Sci. U.S.A. 68*, 2099−2101.
46. Yang, M., and Millar, D. P. (1997) *Methods Enzymol. 278*, 417−444.
47. Vamosi, G., and Clegg, R. M. (1998) *Biochemistry 37*, 14300−14316.
48. Parkhurst, L. J., Parkhurst, K. M., Powell, R., Wu, J., and Williams, S. (2002) *Biopolymers 61*, 180−200.
49. Bailey, M. F., Thompson, E. H. Z., and Millar, D. P. (1900) *Methods 25*, 62−77.
50. Pelletier, H., Sawaya, M. R., Kumar, A., Wilson, S. H., and Kraut, J. (1994) *Science 264*, 1891−1903.
51. Wu, J., Parkhurst, K. M., Powell, R. M., Brenowitz, M., and Parkhurst, J. (2001) *J. Biol. Chem. 276*, 14614−14622.

BI030111L